RSC Advances

PAPER

View Article Online
View Journal | View Issue

Cite this: *RSC Adv.*, 2022, **12**, 35896

Catalytic performance of tridentate *versus* bidentate Co(II) complexes supported by Schiff base ligands in vinyl addition polymerization of norbornene†

Kyeonghun Kim, ‡[a] Saira Nayab,‡[ab] Yerim Cho,[a] Hyewon Jung,[d] Hyeonuk Yeo,[c] Hyosun Lee *[a] and Sang-Ho Lee *[d]

Received 15th November 2022
Accepted 8th December 2022

DOI: 10.1039/d2ra07241f

rsc.li/rsc-advances

A series of Co(II) complexes supported by Schiff base ligands, L_A–L_C, where L_A, L_B, and L_C are (*E*)-3-methoxy-*N*-(quinolin-2-ylmethylene)propan-1-amine, (*E*)-N^1,N^1-dimethyl-N^2-(pyridin-2-ylmethylene) ethane-1,2-diamine, and (*E*)-N^1,N^1-dimethyl-N^2-(thiophen-2-ylmethylene)ethane-1,2-diamine, respectively, were designed and synthesized. Structural studies revealed a distorted trigonal bipyramidal geometry for $[L_BCoCl_2]$ and a distorted tetrahedral geometry for $[L_CCoCl_2]$. After activation with modified methyl aluminoxane (MMAO), all the Co(II) complexes catalyzed the polymerization of norbornene (NB) to yield vinyl-type polynorbornenes (PNBs) with activities of up to 4.69 × 10^4 g_{PNB} mol Co^{-1} h^{-1} at 25 °C. High-molecular-weight (M_n of up to 1.71 × 10^5 g mol^{-1}) soluble PNBs with moderate molecular-weight distributions (MWD) were obtained. The activity of the Co(II)/MMAO catalytic system is influenced by the steric hindrance and electronic properties of the ligands.

Introduction

Polynorbornene (PNB), which is synthesized *via* vinyl addition polymerization, has received considerable attention because of its fascinating properties that stem from its saturated bicyclic backbone.[1] The NB skeleton confers a high thermal stability, low dielectric constant, and high optical transparency, which are attractive characteristics for applications in microelectronics and optics.[1–4] Both early and late transition metal complexes have been reported as active catalysts for the vinyl addition polymerization of NB.[1,5–11] Recently, promising catalytic activities have also been reported for late transition metal catalysts, such as Pd- and Ni-based catalysts.[12–15]

The choice of ancillary ligand significantly affects the catalytic performance of the metal-based initiators in a polymerization reaction.[16–19] Imine-derived ligands are considered privileged because of their structural flexibility, fine tunability, and selectivity toward metal atoms that enable the construction of attractive geometries, ranging from *N*,*N*′-bidentate to *N*,*N*′,*X*-tridentate and *N*,*N*′,*N*,*X*′-tetradentate.[20,21] For instance, a variety of imine-derived Pd(II) modified methyl aluminoxane (Pd(II)/MMAO) systems have displayed high activities toward NB polymerization with effective control of the resultant PNB properties.[4,20,22] Numerous studies on NB polymerization conducted with Co(II) complexes have reported moderate activities.[23–26] The Wang group studied a 2-((3,5-dimethyl-1*H*-pyrazol-1-yl)methyl) pyridine}$CoCl_2$ system that afforded only 31% yield and PNB with an M_n value of 6.05 × 10^3 g mol^{-1}.[27] Similarly, a 2,6-bis[1-(2,5-ditertbutylphenylimino)ethyl] pyridine-derived Co(II) system exhibited an activity of 11.4 × 10^3 g_{PNB} mol Co^{-1} h^{-1} at 30 °C after 12 h.[28] The Frederic group studied a $CoCl_2$ and pyridine bis(imine)Co(II)/MAO system for NB polymerization that resulted in high-molecular-weight PNB (M_n = 4.2 × 10^5 g mol^{-1}).[29] The Sato group studied Co(II) complexes activated with d-MAO, which resulted in 99% yield within 3 h in chlorobenzene at room temperature and yielded low-molecular-weight PNB (3.2 × 10^4 g mol^{-1}).[30] However, the aforementioned complexes were only synthesized in 5% yield when MAO was used for activation.

Recently, we reported a square pyramidal Co(II) complex with an iminomethylpyridine-derived Schiff base ligand (L_A) as an effective catalyst for syndio-enriched poly(methyl methacrylate) MMA polymerization with an activity of up to 4.48 × 10^4 g PMMA mol Co^{-1} h^{-1} and synthesized high-molecular-weight

[a]*Department of Chemistry and Green-Nano Materials Research Center, Kyungpook National University, Daegu, 41566, Republic of Korea. E-mail: hyosunlee@knu.ac.kr*

[b]*Department of Chemistry, Shaheed Benazir Bhutto University, Sheringal Dir (Upper) 18000, Khyber Pakhtunkhwa, Islamic Republic of Pakistan*

[c]*Department of Chemistry Education and Department of Pharmacy, Kyungpook National University, Daegu, 41566, Republic of Korea*

[d]*Center for Advanced Specialty Chemicals, Korea Research Institute of Chemical Technology, Ulsan 44412, Republic of Korea. E-mail: slee@krict.re.kr*

† X-Ray crystallography with PLS-II 2D-SMC beamline was supported by MSIP and POSTECH. CCDC 2178180 and 2178181 contain the supplementary crystallographic data for $[L_BCoCl_2]$ and POSTECH $[L_CCoCl_2]$. For ESI and crystallographic data in CIF or other electronic format see DOI: https://doi.org/10.1039/d2ra07241f

‡ These authors contributed equally to this work.

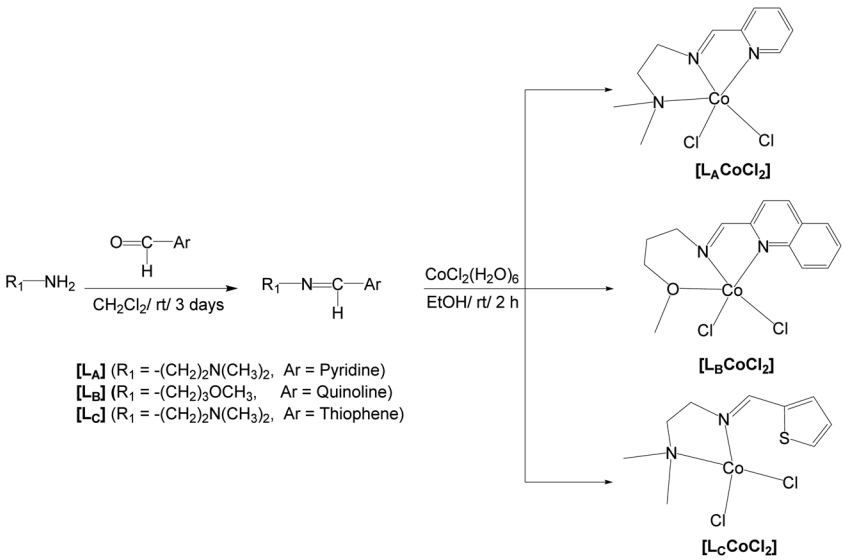

Scheme 1 Scheme illustrating the synthesis of Co(II) complexes, $[L_nCoCl_2]$ ($L_n = L_A$–L_C).

PMMA (11.1×10^5 g mol^{-1}).[31] The same complex, with the *N*,*N*,*N*-coordination mode, exhibited promising results when utilized in the vinyl addition polymerization of NB, which prompted us to explore Co(II) complexes bearing *N*,*N*,*O*-tridentate (L_B) and *N*,*N*-bidentate (L_C) imine ligands with diverse geometries for NB polymerization (Scheme 1). In this work, we present a set of Co(II) complexes with trigonal bipyramidal and tetrahedral geometries for L_B and L_C, respectively, and estimate their catalytic performance in the vinyl addition polymerization of NB. Activation with MMAO resulted in excellent activity, and a Co(II)/MMAO system affording 99% yield in the conversion of NB to PNB within 2 h at 25 °C is reported for the first time. Additionally, the effects of ligand architecture, polymerization temperature, and time on the NB polymerization performance of the studied Co(II) complexes were also investigated.

Experimental section

Materials

$CoCl_2 \cdot 6H_2O$ (Sigma-Aldrich; 98%), 2-pyridinecarboxaldehyde (Sigma-Aldrich; 99%), 2-thiophencaboxaldehyde (Sigma-Aldrich; 99%), 3-metholxypropylamine (Sigma-Aldrich; 99%), bicyclo[2.2.1]hept-2-ene(Sigma-Aldrich; 99%), magnesium sulphate ($MgSO_4$) (Sigma-Aldrich; ≥ 99.5%), 2-quinolinecarbxaldehyde (TCI; 96%), and *N*,*N*′-dimethylethylenediamine (TCI; 98%) were used as received. Anhydrous solvents such as methylene chloride (CH_2Cl_2), ethanol (EtOH), *n*-hexane (*n*-Hex), diethyl ether (Et_2O), 1,2-dichloroethane ($C_2H_4Cl_2$), chlorobenzene, and toluene were purchased from Aldrich Chemicals Corp. and degassed before use. Modified methylaluminoxane (MMAO) was purchased from Lake Materials as 7.10 wt% aluminum in methylcyclohexane solution.

Preparation of Schiff base ligands

(*E*)-N^1,N^1-Dimethyl-N^2-(pyridin-2-ylmethylene)ethane-1,2-diamine (L_A), (*E*)-3-methoxy-*N*-(quinolin-2-ylmethylene)propan-1-amine (L_B), and (*E*)-N^1,N^1-dimethyl-N^2-(thiophen-2-ylmethylene)ethane-1,2-diamine (L_C), were synthesized according to literature procedures.[31–33]

Synthesis of (*E*)-N^1,N^1-dimethyl-N^2-(pyridin-2-ylmethylene) ethane-1,2-diamine cobalt(II) chloride, $[L_ACoCl_2]$

L_ACoCl_2 was synthesized according to the literature.[31]

Synthesis of (*E*)-3-methoxy-*N*-(quinolin-2-ylmethylene)propan-1-amine cobalt(II) chloride, $[L_BCoCl_2]$

A solution of LB (0.228 g, 1.00 mmol) in anhydrous ethanol (10.0 mL) was added to a solution of CoCl2·6H2O (0.238 g, 1.00 mmol) in ethanol (10.0 mL) at room temperature. Precipitation of green solid occurred while stirring the reaction mixture for 12 h. The precipitate was filtered and washed with cold ethanol (50.0 mL × 2). The solid was dried under a vacuum at 60 °C (0.26 g, 72%). X-ray quality crystals of **$[L_BCoCl_2]$** were obtained by the layering of hexane on the CH_2Cl_2 solution of **$[L_BCoCl_2]$**. mp (°C): 191. Analysis calculated for $C_{14}H_{16}Cl_2N_2OPd$ (%): anal. calcd for $C_{14}H_{16}Cl_2CoN_2O$: C, 46.95; H, 4.50; N, 7.82. Found: C, 47.13; H, 4.53; N, 7.88. FT-IR (solid (neat); cm^{-1}): ν(sp^2 C–H) 3016; ν(sp^3 C–H) 2883 m; ν(C=N)imine 1639 m; ν(C=N)quinoline 1554 m; ν(C=C)quinoline 1456 m; ν(C–O) 1090 m; ν(M–N) 564 m.

Synthesis of (*E*)-N^1,N^1-dimethyl-N^2-(thiophen-2-ylmethylene) ethane-1,2-diamine cobalt(II) chloride, $[L_CCoCl_2]$

A method analogous to that used to prepare **$[L_BCoCl_2]$** was adopted for the synthesis of **$[L_CCoCl_2]$**; in this case, L_C (0.364 g, 2.00 mmol) and $CoCl_2 \cdot 6H_2O$ (0.476 g, 2.00 mmol) used to yield the final product (0.46 g, 75%). X-ray quality crystals of **$[L_CCoCl_2]$** were obtained by layering hexane on the CH_2Cl_2 solution

of **[L_CCoCl$_2$]**. mp (°C): 200. Anal. calcd for $C_9H_{14}Cl_2CoN_2S$: C, 34.63; H, 4.52; N, 8.98; S, 10.27. Found: C, 34.66; H, 4.54; N, 8.87; S, 10.45. FT-IR (solid (neat); cm^{-1}): ν(sp^2 C–H) 2976; ν(sp^3 C–H) 2901 m; ν(C=N)$_{imine}$ 1653 s; ν(C=C)$_{thiophene}$ 1454 m; ν(C–S) 857 m; ν(M–N) 588 m.

General polymerization procedure

The polymerization was conducted by applying the Schlenk technique under argon in the flame-dried flask. In the general polymerization procedure, the flask was charged with 15 mmol of NB and 15 μmol of catalyst in 20 mL of solvent (chlorobenzene, toluene, or dichloroethane). The reaction mixture was stirred for 5 min at prescribed temperatures, followed by the addition of MMAO (3.10 mL of 7.10 wt% in methylcyclohexane) under a dry argon atmosphere. The flask was sealed and stirred for the prescribed time. After the prescribed time, the reaction was terminated by the addition of acidic ethanol (200 mL; HCl 1%). The resulting precipitated polymer was collected by filtration, washed with ethanol, and dried overnight under vacuum at 80 °C and characterized by SEC.

Measurements

The NMR spectra of ligands were recorded on a Bruker Avance III (500 MHz for ^{1}H NMR, 125 MHz for ^{13}C NMR) spectrometer. The chemical shifts are recorded in ppm units (δ) using $SiMe_4$ as an internal standard; coupling constants (J) are reported in Hertz (Hz). The Fourier-transform infrared (FT-IR) spectra of synthesized ligands and their corresponding Co(II) complexes were recorded on Bruker FT/IR-Alpha (neat) and data were reported in reverse centimeter (cm^{-1}). Elemental analysis (C, H, N) of the synthesized Co(II) complexes were performed on an elemental analyzer (EA 1108; Carlo-Erba, Milan, Italy). Melting points of synthesized Co(II) complexes, [L_nCoCl$_2$] (L_n = L_A–L_C), were determined with an IA9100 (Electrothermal) instrument. 1H NMR spectrum of PNB demonstrating the absence of double bonds was recorded using Avance III-500 MHz spectrometer, confirming the vinyl-type polymerization of NB. The FT-IR of the resultant PNB was determined using Bruker FT/IR-Alpha (neat), and the representative FT-IR spectra are given in ESI.† The number-average molecular weights (M_n), weight-average molecular weights (M_w), and polydispersity indices (PDI = M_w/M_n) of the obtained PNB samples were determined by size exclusion chromatography (SEC, ACQUITY APC XT, Waters Corp., USA) using chloroform as the eluent at 0.6 mL min^{-1}, with the column temperature set to 40 °C. M_n, M_w, and PDI values were calculated against polystyrene standards.

X-ray crystallographic studies

The X-ray-quality single crystal was coated with paratone-*N* oil and the diffraction data was measured with different levels of synchrotron radiation: the crystal of **[L_BCoCl$_2$]** with synchrotron radiation λ = 0.650 Å at 293(2) K and **[L_CCoCl$_2$]** with synchrotron radiation λ = 0.630 Å at 220(2) K. All crystals on an ADSC Quantum-210 detector at 2D SMC with silicon (111) double crystal monochromator (DCM) at the Pohang Accelerator Laboratory, South Korea. The PAL BL2D-SMDC program[34] was used for data collection (detector distance is 63 mm, omega scan; $\Delta\omega$ = 3°, exposure time is 1 s per frame) and HKL3000sm (Ver. 703r)[35] was used for cell refinement, reduction, and absorption correction. Structures were solved by direct method and refined by full-matrix least-squares refinement using the SHELXL-2018 (ref. 36) computer program. The positions of all non-hydrogen atoms were refined with anisotropic displacement factors. All hydrogen atoms were placed using a riding model, and their positions were constrained relative to their parent atoms using the appropriate HFIX command in SHELXL-2014. X-ray crystallography with PLS-II 2D-SMC beamline was supported by MSIP and POSTECH. Data collection and integration were performed with SMART and SAINT-Plus software packages.[37] Semiempirical absorption corrections based on equivalent reflections were applied by SADABS.[38] Structures were solved by direct methods and refined using a full-matrix least-squares method on F^2 using SHELXTL.[39] All non-hydrogen atoms were refined anisotropically. Hydrogen atoms were added to their geometrically ideal positions. Crystallographic refinements and structural data are summarized in Table S1.†

Results and discussion

Design of Schiff base ligands and coordination patterns of Co(II) complexes

To promote catalytic activity by leveraging the structural differences of Co(II) complexes, Schiff base imine ligands for the Co(II) complex were prepared *via* condensation of various amines with the corresponding aromatic aldehydes, as illustrated in Scheme 1. The obtained ligands were purified by vacuum distillation, and their chemical structures were successfully confirmed by nuclear magnetic resonance (NMR) (Fig. S1–S6†) and Fourier transform infrared (FT-IR) spectroscopic analyses (Fig. 1, S7 and S8†).

Ligands bearing nitrogen with different hybridizations are easily ligated to the metal center. In this regard, Co(II) readily accepts Schiff base ligands (L_n) upon mixing with $CoCl_2 \cdot 6H_2O$ to form monomeric complexes [L_nCoCl$_2$] (L_n = L_A–L_C) in high yields (72–75%). The chemical structures of the obtained Co(II) complexes were confirmed using spectroscopic techniques (Fig. 1 and S7–S8†). For example, a comparison of the FT-IR spectra of the ligands (L_n = L_A–L_C) with those of the complexes [L_nCoCl$_2$] (L_n = L_A–L_C) revealed a slight shift of the ν(C=N) peak to a lower frequency, indicating that complexation was achieved through the bonding of imine nitrogen and the M(II) center.[31,32,40] For instance, the C=N band appeared at 1633 cm^{-1} for L_C, whereas it appeared at 1618 cm^{-1} for **[L_C-CoCl$_2$]**. The C=N bond became weaker upon chelation because of the inductive effect resulting from the sharing of the lone electron pair on the imine nitrogen with the M(II) center.[41] The ligation of ligands to metal ions through the nitrogen atom was also confirmed by the presence of new bands at 608, 565, and 566 cm^{-1} assigned to ν(M–N).[40,42,43] The vibration peak observed in the 1453–1425 cm^{-1} region is assigned to symmetrical and asymmetrical ν(C=C) stretching vibrations of the thiophene ring.[44,45] In the present study, ν(C–O) and (C–S) stretching

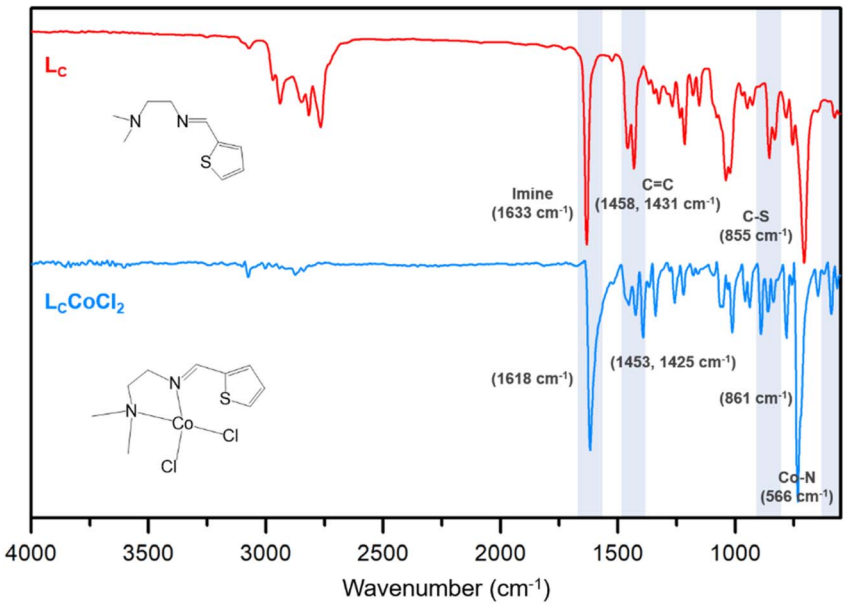

Fig. 1 FT-IR spectra of L_C (top) and $[L_CCoCl_2]$ (bottom).

vibrations were observed at 1040 and 861 cm^{-1}, respectively, in the FT-IR spectra of Co(II) complexes.[31,45–47]

These complexes were stable under atmospheric conditions and could be stored for months at room temperature without deterioration. The purity of the complexes $[L_nCoCl_2]$ ($L_n = L_A$–L_C) was verified by performing composition analysis (%) of the C, H, and N constituents, and good correlations between the calculated and observed values were found (Fig. S9†).

Structural analyses of obtained Co(II) complexes depending on the Schiff base imine ligands by X-ray crystallographic study

Single-crystal X-ray diffraction studies were performed to determine the geometries of the Co(II) complexes. ORTEP diagrams for $[L_BCoCl_2]$ and $[L_CCoCl_2]$ are shown in Fig. 2, and the selected bond lengths and angles are listed in Table S2.†

Five-coordinate $[L_ACoCl_2]$ had a square pyramidal geometry around the Co(II) metal center, whereas the coordination environment around the Co(II) center with five-coordinate $[L_BCoCl_2]$ was distorted trigonal bipyramidal and was obtained *via* coordination with the nitrogen atoms of the quinoline and azomethine moieties and the oxygen atom of the methoxy functionality of L_B. The same is evident from a comparison of the geometric parameter (τ_5) for the five-coordinate complexes; complexes $[L_ACoCl_2]$, and $[L_BCoCl_2]$ coordinated with *N*,*N*,*N*- and *N*,*N*,*O*-tridentate ligands, respectively, and adopted square pyramidal and trigonal bipyramidal geometries (Table 1).[31] The τ_5 parameter is one and zero for perfect trigonal bipyramidal and perfect square pyramidal, respectively.[48,49] Based on the τ_5 values, the geometry of $[L_BCoCl_2]$ is more distorted than that of $[L_ACoCl_2]$.

The Co–$N_{quinoline}$ and Co–N_{imine} bond lengths in $[L_BCoCl_2]$ were 2.1827(12) and 2.0509(12) Å, respectively. The fact that the Co–$N_{quinoline}$ bond is longer than the Co–N_{imine} bond is probably due to the difference in basicity between the quinoline and

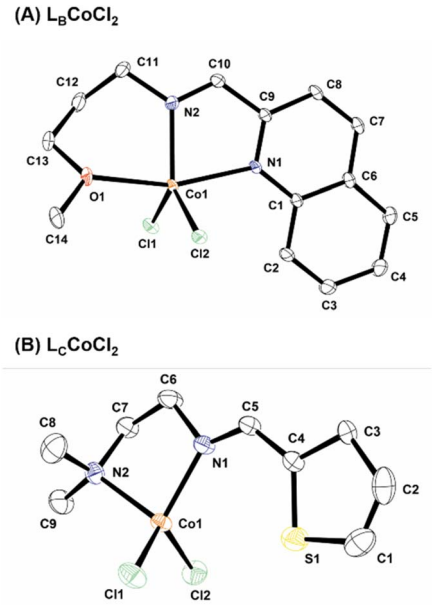

Fig. 2 An ORTEP diagram of (A) $[L_BCoCl_2]$ and (B) $[L_CCoCl_2]$ with thermal ellipsoids at 50% probability. All hydrogen atoms have been omitted for clarity.

imine nitrogen atoms. These structural parameters agree well with the finding that the imine M(II) complexes have a trigonal bipyramidal structure.[43] Additionally, oxygen is also coordinated with the Co(II) center with a bond length of 2.212(12) Å, which is in contrast with the pyridine-derived Co(II) complexes previously studied.[31] The average bond length of Co–Cl was 2.2723 Å, which was within the usual range for Co(II) complexes.[28] The double imine (N=C) bond distances of 1.2798(17) and 1.278(3) Å for $[L_BCoCl_2]$ and $[L_CCoCl_2]$,

Table 1 Five-coordinate geometry indices (τ_5) for **[L_ACoCl$_2$]** and **[L_BCoCl$_2$]** and four-coordinate geometry indices (τ_4) for **[L_CCoCl$_2$]** with representative examples from the literature

Complexes	Geometry	τ_5	τ_4	References
Trigonal bipyramidal (D_{3h})	Trigonal bipyramidal	1.00		48 and 49
[L_ACoCl$_2$]	Square pyramidal	0.10		31
[L_BCoCl$_2$]	Trigonal bipyramidal	0.62		This work
[(bpma)Co(μ–Cl)Cl]$_2$[a]	Trigonal bipyramidal	0.776		43
[(mpme)CoCl$_2$][b]	Square pyramidal	0.414		31
[(dppd)CoCl$_2$][c]	Square pyramidal	0.025		31
Square pyramidal (C_{4v})	Square pyramidal	0.00		48 and 49
Square planar (D_{4h})	Square planar		0.00	50
[L_CCoCl$_2$]	Tetrahedral		0.88	This work
[(pmha)PdCl$_2$][d]	Square planar		0.07	32
Tetrahedral (T_d)	Tetrahedral		1.00	50

[a] [bpma] = 4-bromo-*N*-((pyridin-2-yl)methylene)benzenamine. [b] [mpme] = (*E*)-2-morpholino-*N*-(pyridin-2-ylmethylene)ethanamine. [c] [dppd] = (*E*)-N^1,N^1-dimethyl-N^3-(pyridin-2-ylmethylene)propane-1,3-diamine. [d] [pmha] = (*E*)-*N*-(pyridin-2-ylmethylene)hexan-1-amine.

respectively, agree well with the reported values for Co(II) complexes.[30] The C(9)–C(10) and C(4)–C(5) bond distances of 1.4739(19) and 1.442(4) Å, respectively, for **[L_BCoCl$_2$]** and **[L_CCoCl$_2$]**, respectively, also fall within the usual range, which is indicative of delocalized π-electrons.[43] The N_{imine}–Co–$N_{quinoline}$ (107.14(4)°) bond angle for the five-membered ring was comparable to, albeit slightly larger than, that reported for the Co(II) complex. The N_{oxygen}–Co–N_{imine} and $Cl_{terminal}$–Co–$Cl_{terminal}$ bond angles in **[L_BCoCl$_2$]** were 118.68(3)° and 11.11(1)°, respectively.[30]

The geometry of **[L_CCoCl$_2$]** can be best described as distorted tetrahedral and is obtained *via* coordination with the *N*,*N*-bidentate ligand, and two chloro ligands. The bond lengths of Co–N_{imine} and Co–N_{amine} are 2.040(2) and 2.078(2) Å, respectively. As shown in Table 1, the average Co–Cl and –N=C distances of 2.2239(9) and 1.278(3) Å, respectively, are within the acceptable range, respectively.[31] The τ_4 value is proposed as a simple metric for quantitatively evaluating the geometry of four-coordinated complexes (Table 1).[50] Complexes with an ideal square planar geometry are characterized by a τ_4 value of zero, whereas a τ_4 value of one is characteristic of ideal tetrahedral geometry. The τ_4 parameters of **[L_CCoCl$_2$]** were compared in the reported work and found to be distorted tetrahedral.[31,50] Additionally, the angle between the five-membered *N*,*N*′ chelating ring and thiophene ring in **[L_CCoCl$_2$]** was 17.04(3)°.

The ligand topologies around the Co(II) center were visualized and calculated using the SambVca 2.1 program.[51] The steric maps showed that **[L_ACoCl$_2$]** with a pyridine moiety exhibited a crowded environment around the Co(II) center with a V_{bur} value of 51.0%, whereas **[L_BCoCl$_2$]** with a quinoline-derived ligand showed a V_{bur} value of 51.1%. **[L_CCoCl$_2$]** exhibited the least crowded environment with V_{bur} 46.6%. Topographic steric maps of [[L_nCoCl$_2$] (L_n = L_A–L_C)] illustrating the steric bulk of the attached ligands around the metal center are shown in Fig. 3.

The catalytic activity of Co(II) complexes for the vinyl addition polymerization of NB

To compare the catalytic reactivity for NB polymerization, three Co(II) complexes were examined as catalysts in conjunction with MMAO as a co-catalyst (Fig. 4 and Table 2). The two Co(II) complexes, **[L_BCoCl$_2$]** and **[L_CCoCl$_2$]**, proved to be highly active and produced PNB with a higher yield than **[L_ACoCl$_2$]** at a [NB]/[Al]/[Co] ratio of 1000 : 500 : 1 in chlorobenzene at 25 °C. However, **[L_CCoCl$_2$]** clearly showed faster propagation in the early stages of polymerization and afforded a narrower molecular weight distribution (MWD) with a higher molecular weight of PNB. The obtained PNB was further analyzed by NMR for structural analysis (Fig. S10 and S11†), and the FT-IR spectra of PNB showed no signals at 1620–1680, 966, and 760 cm^{-1},

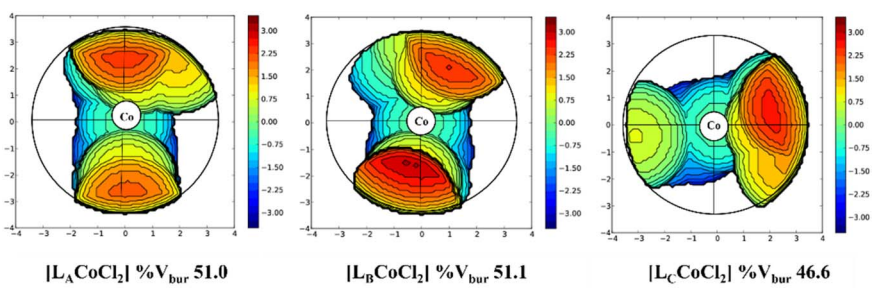

Fig. 3 Topographic steric maps of Co(II) complexes, [L_nCoCl$_2$] (L_n = L_A–L_C).

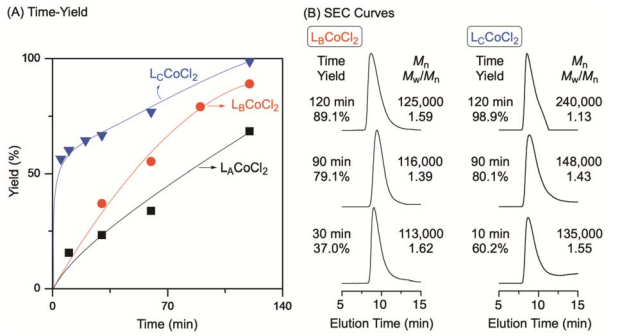

Fig. 4 (A) Time–yield plots and (B) size exclusion chromatography curves for the polymerization of NB with $[L_nCoCl_2]$ (L_n = L_A–L_C) in chlorobenzene at 25 °C: $[Monomer]_0/[MMAO]_0/[Co(II)\ catalyst]_0$ = 650 mM/325 mM/0.65 mM in 20 mL chlorobenzene.

indicating that NB was polymerized by vinyl addition (Fig. S12†).[32,52]

A comparison of catalyst efficiencies showed that the **[L_C-$CoCl_2$]** complex had the highest catalytic activity (4.69×10^4 g_{PNB} mol Co^{-1} h^{-1}) at 25 °C. Under identical experimental conditions, the activities of the Co(II) complexes decreased in the following order: **[L_CCoCl_2]** > **[L_BCoCl_2]** > **[L_ACoCl_2]** (Table 2). From the polymerization results, the effect of the catalyst structure on NB polymerization is apparent. For instance, Co(II) complexes bearing *N*,*N*-bidentate ligands exhibited higher activities than those bearing *N*,*N*,*N*- and *N*,*N*,*O*-tridentate ligands. These results agree with previous reports, where sterically demanding substituents around the metal center negatively affected NB polymerization. The presence of bulky substituents hinders the facile coordination of the bulky NB monomer with the active site, resulting in a decrease in activities.[53–55] Similarly, the difference in the activities of **[L_A-$CoCl_2$]** and **[L_BCoCl_2]**, which have tridentate ligands and almost the same buried volumes (Fig. 3), is apparent (Table 2); the quinoline moiety-bearing catalyst exhibited higher activities than the Co(II) catalyst complexes bearing pyridine-based ligands. These results agree well with our recent reports on Pd(II) complexes bearing amino-methylpyridine and amino-methylquinoline derivatives.[53]

Co(II) coordinates with the nitrogen atoms of the ligand *via* a lone pair of electrons. The ease of availability of these lone pairs controls the net positive charge on the metal center, *i.e.*, the higher the basicity of nitrogen and better the electron availability, the stronger will be the Co–N bond, as is evident from the $Co–N_{quinoline}$ (2.1827(12) Å) and $Co–N_{pyridine}$ (2.1610(1) Å) bond lengths. This scenario can result in a slightly less electropositive metal center for monomer addition. The quinoline ring, which is less basic than pyridine, could exert a more diverse steric and electronic environment on the reactive center than the pyridine ring, providing a more electropositive Pd(II) center. Generally, the transition metal complexes with ligands which made the metal center more electron deficient exhibited higher activities as the olefin could easily coordinate to the electron-deficient metal center.[56] On the other hand, bulky substituted ligands attached to the transition metal complexes are of great benefit to the polymerization, because the bulky moieties can either protecting the metal center and manipulating β-H elimination is inhibited in the polymerization process. These results indicated the apparent but irregular influences of the steric and electronic effects, originating from the collaborations of basicity and steric bulk of ligand substituents. This phenomenon has been supported by recent work by Shi and Jin group, demonstrating the steric hindrance and electronic effect of on the catalytic properties of Pd and Ni complexes.[56,57] Thus, not only the steric hindrance but also the electronic properties of ligands have a significant influence on catalytic performance.

To investigate the optimal reaction parameters for the polymerization of NB using the $[L_nCoCl_2]$/MMAO system, polymerization was performed under various conditions, such as different [Al]/[Co] ratios, temperatures, polymerization times, and solvents (Table 2, Fig. S13 and Table S3–S5†). The polymer yield and catalytic activity depended on the reaction conditions, and polymerization at 25 °C with a [NB]/[Al]/[Co] ratio of 1000 : 500 : 1 was found to be the most effective. The co-catalyst MMAO plays an important role in forming an active species, *i.e.*, maintaining active catalyst precursors as well as forming catalytically active cation–anion ion pairs.[57,58] In the absence of MAO, the chloride complexes were inactive for NB polymerization due to the lack of a cationic M^+–C center for the initiation and propagation steps of polymerization.[57] The catalytic activity of **[L_BCoCl_2]** sharply increased from 0.3 to 3.48×10^4 g_{PNB} mol Co^{-1} h^{-1} on increasing the [Al]/[Co] ratio from 100 to 400 (Table S3†). The highest catalytic activity (4.22×10^4 g_{PNB} mol Co^{-1} h^{-1}) was achieved when the ratio of [Al]/[Co] was increased to 500 (Table S3,† entry 5). Excess MMAO is desirable for polymerization, which might be due to the scavenging of impurities and regeneration of the active species deactivated by transformation/elimination in the system.[58–60] However, a further increase in the MMAO concentration had a negative effect on NB polymerization. Although the polymerization mechanism is no obvious at this point, however the polymerization should start with the formation of a metal alkyl complex as the catalytically active species generated by the reaction of metal complex with MAO. The norbornene monomer occupies the coordination site, and the norbornene would insert into the M–C bond; a repetition of the coordination insertion steps leads to polymer chain growth. Generally, the catalytic species with decrease electron density on the N atom, leading to rapider insertion of monomer.[61,62]

Temperature is another crucial parameter for controlling the NB polymerization progress, in addition to the use of MMAO. When NB polymerization was conducted at 0 °C using **[L_C-$CoCl_2$]**, PNB was obtained in 86.4% yield (Table 2, entry 7). The PNB yield and activity increased appreciably, with the yield increasing from 86.4% to 98.9% and the activity for **[L_CCoCl_2]** increasing from 4.09×10^4 g_{PNB} mol Co^{-1} h^{-1} to 4.69×10^4 g_{PNB} mol Co^{-1} h^{-1}, when the polymerization temperature was increased up to 25 °C (Table 2, entry 8). However, when the temperature exceeded 40 °C, a decrease in the catalytic activity compared to that at 25 °C was observed, indicating the importance of a suitable polymerization temperature for this Co(II)/

Table 2 NB polymerization by Co(II) complexes in the presence of MMAO at various temperatures

Entry	Catalyst[a]	Temp. (°C)	Yield[b] (%)	Activity[c] (g mol Cat^{-1} h^{-1})×10^4	M_n[d] (g mol^{-1})	M_w/M_n[d]
1	$[L_ACoCl_2]$	0	82.5	4.09	125 000	1.59
2	$[L_ACoCl_2]$	25	72.7	3.44	120 000	1.65
3	$[L_ACoCl_2]$	40	59.0	2.79	75 000	2.08
4	$[L_BCoCl_2]$	0	85.2	4.04	181 000	1.39
5	$[L_BCoCl_2]$	25	89.1	4.22	125 000	1.59
6	$[L_BCoCl_2]$	40	67.9	3.22	74 000	1.79
7	$[L_CCoCl_2]$	0	86.4	4.09	121 000	1.63
8	$[L_CCoCl_2]$	25	98.9	4.69	240 000	1.13
9	$[L_CCoCl_2]$	40	59.0	2.79	177 000	1.29

[a] $[NB]_0/[MMAO]_0/[Co(II)\ catalyst]_0$ = 650 mM/325 mM/0.65 mM in chlorobenzene 20 mL at 25 °C for 2 h. [b] Yield is defined as (a mass of dried polymer recovered)/(a mass of monomer used). [c] Activity is a g_{PNB} mol Co^{-1} h^{-1}. [d] Measured *via* SEC calibrated with PS standards in chloroform (40 °C, flow rate 1.0 mL min^{-1}).

MMAO system. No clear trends in the M_n values and MWD with decreasing polymerization temperature were observed for the $[L_nCoCl_2]$/MMAO system (Table 2). It is not difficult to realize that the rate of monomer consumption and the resultant PNB yield increased with polymerization time, while the catalytic activity decreased because the rate of catalysis was slowed down due to the viscosity of the converted PNB (Table S3†).[63] For example, in the case of $[L_CCoCl_2]$, the activity dropped from 64.1× 10^4 g_{PNB} mol Co^{-1} h^{-1} at 5 min to 4.69× 10^4 g_{PNB} mol Co^{-1} h^{-1} at 120 min (Table S4,† entries 1 and 7).

The polarity of the solvent also has a significant effect on the activity of the $[L_nCoCl_2]$/MMAO (L_n = L_A–L_C) system for PNB synthesis. An increase in the relative polarity of the solvent from toluene (polarity 0.099) to chlorobenzene (0.188) resulted in a significant increase in the PNB yield at 25 °C. A further increase in the polarity of the solvent, *i.e.*, using 1,2-dichloroethane (0.327) as the polymerization solvent, had a detrimental effect on the catalytic performance of the $[L_nCoCl_2]$/MMAO (L_n = L_A–L_C) system. Thus, the appropriate choice of polymerization solvent with optimal polarity is crucial for controlling NB polymerization (Table S5†). Polymerization in toluene was carried out at 80 °C and yields of 65–70% were obtained, indicating that the Co(II) catalysts had reasonable thermal stability.

The Co(II) system reported herein exhibited a higher yield (98% within 2 h) with a lower co-catalyst concentration ([Al]/[Co] ratio of 500 : 1) at 25 °C than a recently reported Pd(II) complex bearing tridentate quinoline-based ligands (76% yield within 5 min with a Al/Pd ratio of 5000 : 1), although the activity of our system was slightly lower (Table 2).[64] Similarly, compared to the $[L_nCoCl_2]$/MMAO system reported here, a recently studied cationic acetylacetonate bis(secondary amine) Pd(II) complex displayed a higher activity (1.3 × 10^5 g_{PNB} mol Pd^{-1} h^{-1}) but a lower yield (56% in 4 h) for vinyl-type NB polymerization in the presence of 25 eq. $BF_3{\cdot}OEt_2$ as the co-initiator.[65]

Conclusions

A series of Co(II) complexes based on *N*,*N*,*N*- and *N*,*N*,*O*-tridentate and *N*,*N*-bidentate Schiff base ligands were studied. The geometries around the Co(II) center in $[L_BCoCl_2]$ and $[L_CCoCl_2]$ can be described as distorted trigonal bipyramidal and distorted tetrahedral, respectively. To optimize the polymerization of NB by the $[L_nCoCl_2]$/MMAO system, various polymerization conditions were investigated. Upon activation with MMAO, the Co(II) complexes served as promising catalysts for the vinyl-type polymerization of NB. Catalytic activities of up to 4.69 × 10^4 g_{PNB} mol Co^{-1} h^{-1} at 25 °C were demonstrated by $[L_nCoCl_2]$/MMAO in chlorobenzene. This system represents the first example of a Co(II)/MMAO system yielding 99% yield at 25 °C. It has been demonstrated that the steric hindrance and electronic properties of ligand architectures influence their catalytic properties.

Author contributions

K. Kim and S. Nayab contributed equally to this work. The manuscript was written through the contributions of all authors. All authors have given approval for the final version of the manuscript.

Conflicts of interest

The authors declare no competing financial interest.

Acknowledgements

This research was supported by the National Research Foundation (NRF) of Republic of Korea, funded by the Ministry of Education, Science, and Technology (MEST) (Grant No. 2019R1A2C1088654). This work was also supported by the Technology Innovation Program (TIP # 20011123, Development of Cyclic Olefin Polymer (COP) with High Heat Resistance and High Transmittance) funded by the Korea Evaluation Institute of Industrial Technology (KEIT) and the Ministry of Trade, Industry & Energy (MOTIE, Republic of Korea).

Notes and references

1 F. Blank and C. Janiak, *Coord. Chem. Rev.*, 2009, **253**, 827–861.

2 I. V. Nazarov, E. V. Bermesheva, K. V. Potapov, Z. B. Khesina, M. M. Il'in, E. K. Melnikova and M. V. Bermeshev, *Mendeleev Commun.*, 2021, **31**, 690–692.
3 K. H. Park, R. J. Twieg, R. Ravikiran, L. F. Rhodes, R. A. Shick, D. Yankelevich and A. Knoesen, *Macromolecules*, 2004, **37**, 5163–5178.
4 T. Zheng, H. Liao, J. Gao, L. Zhong, H. Gao and Q. Wu, *Polym. Chem.*, 2018, **9**, 3088–3097.
5 C. Janiak and P. G. Lassahn, *J. Mol. Catal. A: Chem.*, 2001, **166**, 193–209.
6 W. Kaminsky and A. Laban, *Appl. Catal., A*, 2001, **222**, 47–61.
7 L. Boggioni, H. Harakawa, S. Losio, K. Nomura and I. Tritto, *Polym. Chem.*, 2021, **12**, 4372–4383.
8 Y. Li, L. Jiang, L. Wang, H. Gao, F. Zhu and Q. Wu, *Appl. Organomet. Chem.*, 2006, **20**, 181–186.
9 B. L. Goodall, W. Risse and J. P. Mathew, WO1995014048A1, 1996.
10 D. A. Barnes, G. M. Benedikt, B. L. Goodall, S. S. Huang, H. A. Kalamarides, S. Lenhard, L. H. McIntosh, K. T. Selvy, R. A. Shick and L. F. Rhodes, *Macromolecules*, 2003, **36**, 2623–2632.
11 C. Chen, *Nat. Rev. Chem.*, 2018, **2**, 6–14.
12 J. Dong, D. Yang and B. Wang, *Eur. J. Inorg. Chem.*, 2021, **2021**, 4661–4668.
13 D. Yang, Y. Tang, H. Song and B. Wang, *Organometallics*, 2016, **35**, 1392–1398.
14 X. Wang, B. Dong, Q. Yang, H. Liu, Y. Hu and X. Zhang, *Inorg. Chem.*, 2021, **60**, 2347–2361.
15 S. Das, V. Subramaniyan and G. Mani, *Inorg. Chem.*, 2019, **58**, 3444–3456.
16 M. C. Sacchi, M. Sonzogni, S. Losio, F. Forlini, P. Locatelli, I. Tritto and M. Licchelli, *Macromol. Chem. Phys.*, 2001, **202**, 2052–2058.
17 Z. Chen and M. Brookhart, *Acc. Chem. Res.*, 2018, **51**, 1831–1839.
18 W. H. le Roux, M. Matthews, A. Lederer, A. J. van Reenen and R. Malgas-Enus, *J. Catal.*, 2022, **405**, 571–587.
19 F. Wang and C. Chen, *Polym. Chem.*, 2019, **10**, 2354–2369.
20 M. Li, X. Shu, Z. Cai and M. S. Eisen, *Organometallics*, 2018, **37**, 1172–1180.
21 M. Li, X. Shu, Z. Cai and M. S. Eisen, *Polym. Chem.*, 2019, **10**, 2741–2748.
22 J. Long, H. Gao, F. Liu, K. Song, H. Hu, L. Zhang, F. Zhu and Q. Wu, *Inorg. Chim. Acta*, 2009, **362**, 3035–3042.
23 G. Leone, A. Boglia, A. C. Boccia, S. T. Scafati, F. Bertini and G. Ricci, *Macromolecules*, 2009, **42**, 9231–9237.
24 F. P. Alt and W. Heitz, *Macromol. Chem. Phys.*, 1998, **199**, 1951–1956.
25 M. C. Sacchi, M. Sonzogni, S. Losio, F. Forlini, P. Locatelli, I. Tritto and M. Licchelli, *Macromol. Chem. Phys.*, 2001, **202**, 2052–2058.
26 F. Pelascini, F. Peruch, P. J. Lutz, M. Wesolek and J. Kress, *Macromol. Rapid Commun.*, 2003, **24**, 768–771.
27 D. Zhang, Q. Yue, J. Wang, G. Shigeng and L. Weng, *Inorg. Chem. Commun.*, 2009, **12**, 1193–1196.
28 L. L. Benade, S. O. Ojwach, C. Obuah, I. A. Guzei and J. Darkwa, *Polyhedron*, 2011, **30**, 2878–2883.
29 J. Chen, Y. Huang, Z. Li, Z. Zhang, C. Wei, T. Lan and W. Zhang, *J. Mol. Catal. A: Chem.*, 2006, **259**, 133–141.
30 Y. Sato, Y. Nakayama and H. Yasuda, *J. Organomet. Chem.*, 2004, **689**, 744–750.
31 J. Lee, K. Kim, H. Lee and S. Nayab, *Polyhedron*, 2021, **196**, 115003.
32 K. Kim, S. Nayab, A. Rim Jeong, Y. Cho, H. Yeo and H. Lee, *Inorg. Chim. Acta*, 2022, **539**, 121025.
33 C. Anderson, M. Crespo, M. Font-Bardía, A. Klein and X. Solans, *J. Organomet. Chem.*, 2000, **601**, 22–33.
34 J. W. Shin, K. Eom and D. Moon, *J. Synchrotron Radiat.*, 2016, **23**, 369–373.
35 Z. Otwinowski and W. Minor, *Methods Enzymol.*, 1997, 307–326.
36 G. Sheldrick, *Acta Crystallogr., Sect. A: Found. Crystallogr.*, 2008, **64**, 112–122.
37 *SMART and SAINT-Plus v 6.22*, Bruker AXS Inc., Madison, Wisconsin, USA, 2000.
38 G. M. Sheldrick, *SADABS v 2.03*, University of Göttingen, Germany, 2002.
39 *SHELXTL v 6.10*, Bruker AXS Inc, Madison, Wisconsin, USA, 2000.
40 S. Park, J. K. Lee, H. Lee, S. Nayab and J. W. Shin, *Appl. Organomet. Chem.*, 2019, **33**(4), e4797.
41 X.-L. Yang, G.-Q. Zhong and L. Wu, *J. Chem.*, 2013, **2013**, 1–5.
42 S. H. Ahn, S.-I. Choi, M. J. Jung, S. Nayab and H. Lee, *J. Mol. Struct.*, 2016, **1113**, 24–31.
43 S. Park, J. Lee, H. Lee, A. R. Jeong, K. S. Min and S. Nayab, *Appl. Organomet. Chem.*, 2018, **33**, e4766.
44 Y. Mei-Rong, S. Yu and X. Yong-Jin, *SpringerPlus*, 2014, **3**, 701.
45 S. Kulandaivalu, Z. Zainal and Y. Sulaiman, *Int. J. Polym. Sci.*, 2016, **2016**, 1–12.
46 M. Vairalakshmi, R. Princess, B. K. Rani and S. J. Raja, *J. Chil. Chem. Soc.*, 2018, **63**, 3844–3849.
47 S. Chandra and R. Kumar, *Transition Met. Chem.*, 2004, **29**, 269–275.
48 A. W. Addison, T. N. Rao, J. Reedijk, J. van Rijn and G. C. Verschoor, *J. Chem. Soc., Dalton Trans.*, 1984, 1349–1356.
49 D. C. Crans, M. L. Tarlton and C. C. McLauchlan, *Eur. J. Inorg. Chem.*, 2014, **2014**, 4450–4468.
50 L. Yang, D. R. Powell and R. P. Houser, *Dalton Trans.*, 2007, 955–964.
51 L. Falivene, R. Credendino, A. Poater, A. Petta, L. Serra, R. Oliva, V. Scarano and L. Cavallo, *Organometallics*, 2016, **35**, 2286–2293.
52 A. R. Jeong, S. Nayab, E. Kim, H. Yeo and H. Lee, *J. Mol. Struct.*, 2022, **1264**, 133238.
53 H. Yuan, H. Liu, F. You and X. Shi, *Inorg. Chem. Commun.*, 2020, **119**, 108139.
54 J. Deng, H. Gao, F. Zhu and Q. Wu, *Organometallics*, 2013, **32**, 4507–4515.
55 V. Appukuttan, J. H. Kim, C. S. Ha and I. Kim, *Korean J. Chem. Eng.*, 2008, **25**, 423–425.
56 Z.-J. Yao and G.-X. Jin, *Coord. Chem. Rev.*, 2013, **257**, 2522–2535.

57 F. You, H. Liu, G. Luo and X. Shi, *Dalton Trans.*, 2019, **48**, 12219–12227.
58 E. Y.-X. Chen and T. J. Marks, *Chem. Rev.*, 2000, **100**, 1391–1434.
59 W. Kaminsky, *J. Polym. Sci., Part A: Polym. Chem.*, 2004, **42**, 3911–3921.
60 S. D. Ittel, L. K. Johnson and M. Brookhart, *Chem. Rev.*, 2000, **100**, 1169–1204.
61 D. H. Lee, J. H. Lee, G. H. Eom, H. G. Koo, C. Kim and I. M. Lee, *Bull. Korean Chem. Soc.*, 2011, **32**, 1884–1890.
62 Y. M. Xu, K. Li, Y. Wang, W. Deng and Z. J. Yao, *Polymers*, 2017, **9**, 105.
63 H. Liu, H. Yuan and X. Shi, *Dalton Trans.*, 2019, **48**, 609–617.
64 H. Liu, H. Yuan and X. Shi, *Inorg. Chem. Commun.*, 2020, **119**, 108139.
65 H. Liu, H. Yuan and X. Shi, *J. Mol. Struct.*, 2017, **1133**, 411–421.